PCCP

Theoretical study of the valence and core photoemission spectra of C_{60}

P. Colavita, G. De Alti, G. Fronzoni, M. Stener and P. Decleva*

Dipartimento di Scienze Chimiche, Università di Trieste, Via L. Giorgieri 1, I 34127 Trieste, Italy. E-mail: decleva@univ.trieste.it

Received 31st May 2001, Accepted 22nd August 2001
First published as an Advance Article on the web 24th September 2001

The photoionization cross section and angular distribution relative to all primary ionizations in C_{60} have been computed employing a convergent one-centre expansion and an LDA hamiltonian over an extended energy range. The results show the presence of very sharp shape resonances both in the valence and core spectra. Good agreement is obtained with available experimental data, notably the HOMO/HOMO-1 oscillations, the absolute total photoabsorption and the available photoionization spectra, suggesting that more structure should be observable in the low energy region.

Introduction

The C_{60} molecule, being the prototype of an entirely new class of carbon compounds, has been extensively studied, both experimentally and theoretically. Among its spectroscopic properties, photoemission studies are those most directly connected with the electronic structure.

Several calculations of the molecular orbitals and the relevant ionization potentials have been performed[1–14] and photoelectron spectra have been measured at various energies.[7,8,15–25] Cross sections and angular distributions have been obtained. However, because of experimental difficulties, data are rather sparse, and only a few aspects, notably the well-known high energy oscillations in the cross section ratio between the two outermost bands (HOMO and HOMO-1),[16,20–23] have been carefully analysed. Although the exploitation of the full I_h symmetry of C_{60} brings about a large computational saving, it is still a rather large system for high quality quantum chemical calculations, and most structural studies have been performed at the Hartree–Fock or density functional (DFT) levels, or with semiempirical models.[1–14] Calculation of photoemission properties is significantly more difficult, as it involves evaluation of continuum wavefunctions. Here several spherical models have been employed,[26–28] which capture some of the most significant features of the spectra but cannot attain more than a qualitative understanding. Molecular calculations involving plane waves for the final states have been performed,[11,12] and recently a more sophisticated approach based on multicenter atomic waves has been employed,[21,22] obtaining excellent agreement with the experimentally derived profile of the HOMO/HOMO-1 ratio. An important issue is the role of many body effects in photoabsorption and photoemission of C_{60}. Because of the large number of delocalized π electrons it is expected that correlation, or response of the electron cloud to the external perturbation, may be large. Calculations of the low lying excitations employing single excitation configuration interaction (SCI) at the semiempirical level, as well as model RPA and TDLDA calculations of the total photoabsorption,[29–31] have revealed important effects, which are largest below and close to threshold. A full TDLDA calculation has recently appeared[32] employing a novel algorithm based on real time solution of the TDLDA equations, although a large numerical noise is present in the calculated spectrum. Although it is not presently feasible to include response in full continuum calculations on C_{60}, this indicates that results at the LDA level should be treated with caution close to threshold, where large oscillator strength is available.

We have recently developed a large-scale one-center code for the solution of the continuum functions,[33] as a first step of an ongoing effort to obtain high quality solutions for complex molecular systems employing a multicenter expansion. In the case of highly symmetrical systems the full use of symmetry allows the use of very high angular momenta, so that accurate convergence of photoionization profiles may be achieved by a pure one-center expansion even for rather large systems, as is the case of C_{60}.[34] Actually a single center expansion very similar to the present one has been recently employed in the study of electron scattering properties in C_{60}.[35–38] Furthermore a recent study[39] of the LB94 potential,[40] which incorporates the correct asymptotic behaviour and has been designed primarily for the study of polarizabilities, a property closely related to photoabsorption, has shown a significant advantage over the previous VWN transition state (TS) potential which was generally employed.[33] Comparing with the latter it is found that the use of the ground state LB94 potential gives results of comparable or better accuracy, even for the core region. Moreover, this brings also a large computational advantage, since the entire spectrum is obtained with a single state independent potential, making feasible the treatment of the complete spectrum.

So given the fundamental importance of C_{60}, we have considered it interesting to extend our previous exploratory study[34] to cover the entire photoionization spectrum, which includes 32 valence and 16 core ionizations. The results obtained are convergent solutions of the LDA equations, and, with the reservations already noted for the near threshold behaviour, are expected to be capable of highlighting the most important features of the spectra, of which only a small part has been experimentally studied in detail. In fact, apart from the HOMO/HOMO-1 ratio already mentioned,[16,20–23] data for individual cross section profiles and asymmetry parameters are rather few, even if photoelectron spectra taken at different energies clearly show some large intensity changes between different bands. It is generally found that, contrary to the situation common in most small molecules, the cross

section and angular distribution profiles are characterized by the presence of many sharp shape resonances close to threshold, with features extending up to some 40 eV above threshold, in the whole spectrum, including inner valence and core orbitals. This indicates that the photoemission spectra of C_{60} may be more structured than is suggested by the experimental data available, and that even if many overlapping bands are present, large changes in shape and relative intensities could be experimentally detected and more information extracted. Finally, several measurements of absolute total cross section with various techniques have produced widely different results, and a recent critical reassessment of different experimental data, covering an extended energy region, has been presented,[41] asserting the need of a comparable theoretical treatment, and providing an excellent opportunity of comparison with present data.

Computational method

The computational scheme employed has been previously described in detail[33,34] and will be only briefly summarized. A Kohn–Sham hamiltonian

$$h_{KS} = T + V_N + V_C[\rho] + V_{XC}[\rho]$$

is completely defined by the ground state (GS) density ρ and the form of the exchange-correlation potential V_{XC} for which we employ the LB94 functional.[40] The GS density is obtained by a conventional bound state calculation, employing the ADF program[42] with a DZP basis set. The resulting eigenvalue equations

$$h_{KS}\,\varphi = E\varphi$$

are then solved in a single center basis defined as products of *B*-spline radial functions times real spherical harmonics

$$\chi_{ilm} = 1/rB_i(r)Y_{lm}(\theta, \varphi)$$

which are further symmetry adapted to the full molecular point group.

For the bound state initial orbitals a conventional diagonalization is employed, using an iterative scheme, while for the continuum a full set of independent eigenvectors is obtained at each prefixed energy employing the inverse iteration approach to the energy dependent matrix[43]

$$A(E) = H - ES$$

Convergence is determined by the angular momentum expansion, which is very smooth and can be carefully controlled. As we have previously shown[34] very satisfactory convergence can be achieved in C_{60} at $L_{max} = 60$, giving accurate numerical solutions of the LDA equations even in the case of very sharp features which can be followed in detail.

Cross sections and asymmetry parameters are obtained from dipole matrix elements $\langle\varphi_i, r\varphi_E\rangle$ and phase shifts employing the angular momentum transfer formalism.[44]

Results and discussion

Valence region

The electronic structure of C_{60} has been discussed several times,[1–14] and the nature and ordering of the molecular orbitals and IP's may be considered to be well established, except for details within closely spaced levels. In addition to I_h symmetry labels, the quasispherical nature of C_{60} (the first nonspherical potential component is $l = 6$, rather weak, and the first strong component is $l = 10$) makes l a fairly good quantum number for most orbitals,[7,9] as can be seen from the dominating radial component. Moreover, the σ/π symmetry, which is not strict in I_h, is also very well conserved as can be seen in the radial components being symmetric or antisymmetric across the carbon surface.[9]

The IP's calculated by the VWN TS approach are reported in Table 1 together with the proposed assignment to the experimental features.[8] The orbital labels relative to the σ/π character and the dominant angular momentum are also indicated. The present results are also compared with a full valence experimental spectrum in Fig. 1. Apart from the total span of the spectrum, which is slightly underestimated, the agreement is very satisfactory. Comparison with previous DFT[7,9,11,12] and *ab initio* KT results[10] shows good agree-

Table 1 Experimental[8] and calculated valence ionization potentials of C_{60}[a]

Band	EXP[a]	VWN TS	Label[b]		
1	(7.6)	(8.74)	$6h_u$	π	$l = 5$
2	1.4	1.13	$6g_g$	π	4 (+6)
		1.24	$10h_g$	π	4
3	3.2–4.0	2.80	$6g_u$	π	3
		3.10	$5h_u$	σ	9 (+11)
		3.30	$6t_{2u}$	π	3
		3.39	$9h_g$	σ	10 (+8)
4	4.8–6.2	4.42	$5g_u$	σ	9 (+7+11)
		4.58	$8h_g$	π	2
		4.89	$2t_{2g}$	σ	8
		5.16	$5g_g$	σ	8 (+10)
		5.53	$7h_g$	σ	8 (+10)
		5.65	$6t_{1u}$	π	1
		6.01	$4g_u$	σ	7 (+9)
		6.20	$4a_g$	π	0
5	7.2	6.68	$5t_{2u}$	σ	7 (+11)
6	~7.8–9	7.30	$5t_{1u}$	σ	7 (+5+11)
		7.56	$4h_u$	σ	7
		8.30	$4g_g$	σ	6
7	~11	9.49	$3a_g$	σ	6 (+12)
		9.81	$2t_{1g}$	σ	6
		9.96	$6h_g$	σ	6
7′	12	10.99	$4t_{2u}$	σ	5
8	14	12.03	$4t_{1u}$	σ	5
		12.19	$3h_u$	σ	5
9	15	13.68	$3g_g$	σ	4
		14.15	$5h_g$	σ	4
10	~16–19.5	15.42	$3g_u$	σ	3
		16.28	$3t_{2u}$	σ	3
		17.27	$4h_g$	σ	2
		18.23	$3t_{1u}$	σ	1
		18.73	$2a_g$	σ	0

[a] The absolute energy for the first ionization is reported; for all other ionizations relative energies are given. [b] The symmetry in the I_h point group, the σ/π character and the dominant angular momentum l of the wavefunction are indicated.

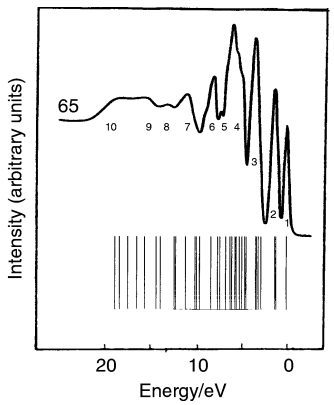

Fig. 1 Full valence experimental photoelectron spectrum of C_{60}[8] and calculated VWN TS ionization potentials.

ment, except for the ordering within band 3 (the relative position of the π and σ levels, which varies widely) and band 4, which consists of 7 or 8 ionizations. In particular the lowest π orbital $4a_g$ (π_0) may be part of band 5.[11,12]

Figs. 2–4 collect the partial cross sections, summed over the relevant ionizations relative to the first three bands, those relative to bands 4, 6 and 7, and those relative to bands 8, 9 and 10, respectively, which are fairly well resolved and therefore should be amenable to a detailed experimental investigation. It has to be noted that the photon energy scale is obtained by adding the VWN TS ionization potentials to the photoelectron kinetic energy.

The most striking feature is the presence of very sharp resonances in the low energy range. These are necessarily shape resonances, since the LDA model employed cannot describe autoionizing states, and are very different from the wide structures present in the photoionization of most small molecules, although the photoelectron spectrum itself is typically molecular, with several well-resolved bands, as has been often noted.[7,9] These resonances are obviously related to the peculiar spherical potential well of the C_{60} cage, we have shown, however, that the nonspherical molecular potential is essential to obtain the proper structures.[34] This is understandable since, in addition to mixing different angular momenta, they induce important changes in the final wavefunction close to the carbon atoms, where most of the contribution to the dipole moment is obtained. The presence of sharp features shows also the importance of a computational scheme able to get a high energy resolution to obtain an accurate photoionization profile from the given model, even if the experimental spectra may be broadened by many electron or vibrational effects presently neglected, or by instrumental resolution. It is also worth observing the very high cross section, in the hundred Mb region, reached close to threshold, for which there is experimental evidence,[17,23] and the presence of additional structures in the spectra up to rather high photon energies. Actually, even sharper resonances are apparent in the individual channel contributions. Since there are many contributions to each composite band we shall not discuss them analytically. A more detailed discussion of the partial contri-

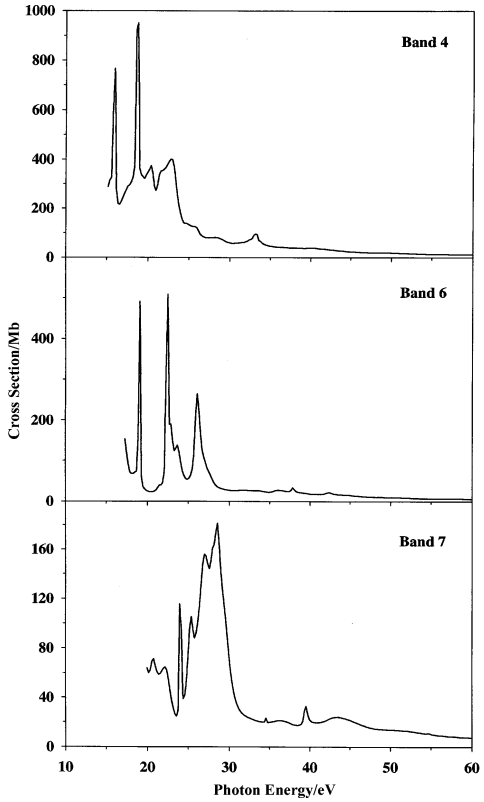

Fig. 3 Calculated cross section profiles relative to bands 4, 6 and (7 + 7′) of C_{60} summed over the relevant ionizations (Table 1). The VWN TS ionization potentials are employed for all ionizations.

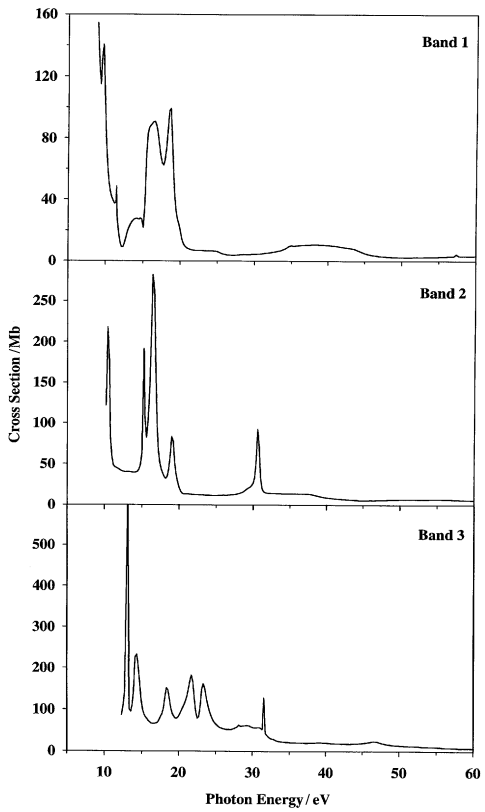

Fig. 2 Calculated cross section profiles relative to the three outermost bands of C_{60} summed over the relevant ionizations (Table 1). The VWN TS ionization potentials are employed for all ionizations.

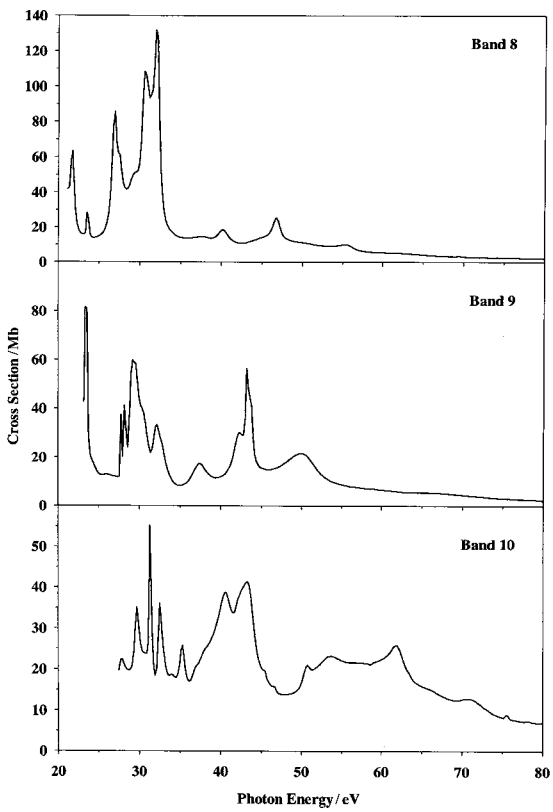

Fig. 4 Calculated cross section profiles relative to bands 8, 9 and 10 of C_{60} summed over the relevant ionizations (Table 1). The VWN TS ionization potentials are employed for all ionizations.

butions to bands 1–3 has been presented in previous work,[34] with the VWN TS potential. We note that the present LB94 potential, being more attractive, shifts the spectra towards threshold, but the general features, as well as the interpretation, remain unchanged. The same general features are also present in the following bands. There are two groups of low energy resonances, the first close to threshold, the second separated by about 5–6 eV. These correspond rather closely to transitions into valence virtual orbitals. For each symmetry (except a_u), the lowest unoccupied valence orbital is π^*, and some of them appear below threshold, notably the $7t_{1u}$, which is the LUMO. The following orbitals are all σ^*, with a gap of about 6–8 eV from the corresponding π^*, clustered in a few groups, the highest being around 18 eV above threshold. Because of the high l values involved, and the associated centrifugal barrier, these antibonding orbitals interact very little with the underlying nonresonant continuum which cannot effectively penetrate at low energy, and so they give rise to exceedingly sharp shape resonances, a dramatic example of the so-called molecular giant resonances first discussed in ref. 45. Unfortunately the high density of states means a large overlap between distinct features. Resonances at still higher energies cannot be associated with antibonding orbitals, they are wider, and are probably due to trapping of high l spherical waves inside the cavity.

Figs. 5 and 6 shows average asymmetry parameters relative to bands 4, 6, 7 and 8, 9, 10, respectively. Those relative to bands 1–3 are essentially similar to those already presented in ref. 32, where rather good agreement with the few experimental data available was observed. Even summing over many contributions relative to the experimental bands leaves pronounced structure on the β profiles, some of which are on a sufficiently wide energy scale to allow an experimental study. The range of β values, on the other hand, span a rather limited range, rarely falling outside the interval 0–1.

The best known feature in the photoionization spectra is the presence of wide oscillations in the two outermost

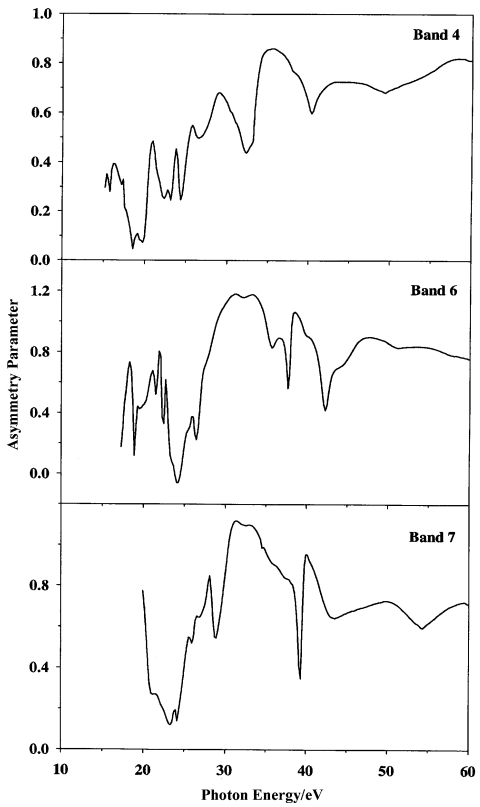

Fig. 5 Calculated asymmetry parameter profiles relative to bands 4, 6 and (7 + 7′) of C_{60} summed over the relevant ionizations (Table 1). The VWN TS ionization potentials are employed for all ionizations.

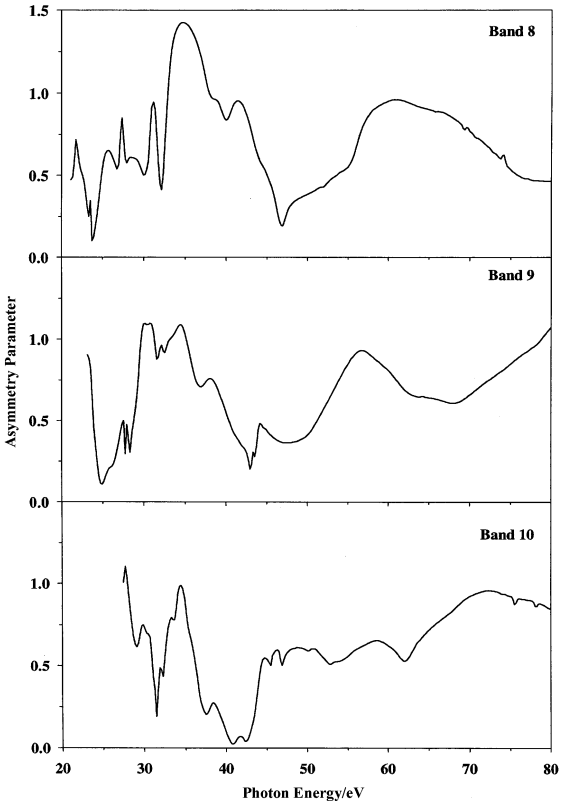

Fig. 6 Calculated asymmetry parameter profiles relative to bands 8, 9 and 10 of C_{60} summed over the relevant ionizations (Table 1). The VWN TS ionization potentials are employed for all ionizations.

bands,[16,20] which has been recently measured with high accuracy over an extended energy range.[21,22] The present results, together with the experimental data and the most accurate theoretical calculations.[21,22] are presented in Fig. 7. As can be seen excellent agreement, including the damping at high energy, is obtained over the whole energy range, after employing a high energy shift of about 4 eV of the calculated profile (upper panel of Fig. 7). This gives confidence in the quality of

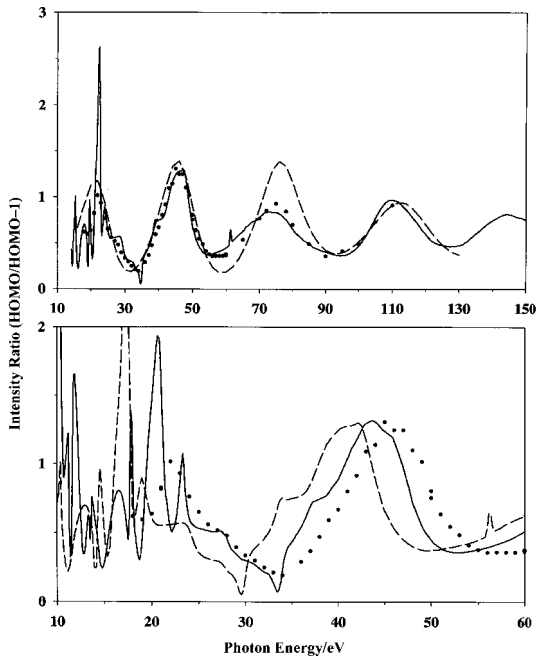

Fig. 7 Upper panel: HOMO/HOMO-1 cross section ratio. (●) experimental values, ref. 21; (– – –) theoretical calculation, ref. 21; (——) present calculation. Lower panel: (●) experimental values (– – –) present calculation; (——) VWN TS results.[34]

the present model for the photoionization profiles, which is purely *ab initio*, without any special parameterization for this particular feature, and is able to give a unified description of the entire spectrum of C_{60}. At the same time this result also gives very clear and quantitative evidence of the fact that the LB94 potential is too attractive, shifting the calculated profiles too close to threshold. This has been generally suggested by previous results in small molecules,[39,46] and is also apparent upon comparing the results obtained for the cross section profiles of the first three bands obtained with the VWN TS potential.[34] Actually the HOMO/HOMO-1 ratio given by the latter is compared with the present result in the lower panel of Fig. 7. As can be seen the two profiles are very similar except for a translation of the VWN TS profile towards higher photon energies, closer to the experimental data, but still too low by a couple of eV. It is to be noted that a similar adjustment of the calculated profile by suitable choice of the inner potential V_0 has been employed in the theoretical results.[21] As an aside this shows the relevance of precise photoionization data to drive improvement in the design of LDA potentials for cross section calculations.

A direct comparison with experimental photoemission data may be obtained by simulating the photoelectron spectra. This has been often made by simply employing the density of states,[7,9] or by the use of cross sections evaluated with plane waves as final states.[11,12] Even if a reasonable qualitative agreement is obtained, it is hardly possible to follow spectral changes with photon energy, especially in the low energy region where many resonances are present and cross sections vary very rapidly. In the present case the fairly good cross section profiles obtained allow to mimic the C_{60} valence spectrum at different photon energies. In Fig. 8 the calculated spectrum at 60 eV photon energy is presented. Convolution with gaussians of width 0.4 eV for the first 5 bands and 1.0 eV for the rest has been employed. Comparison with the experimental spectrum in Fig. 1 shows a fairly satisfactory agreement, although the shape of band 4 is not well reproduced, and band 5 is somewhat too intense. We note that the choice of widths has a marked influence on the visual appearance of the spectrum, and that experimental bands often have an asymmetric shape. The structure of band 4 is worth further discussion. In our results (see Table 1) it comprises eight ionizations, and it is meaningless to report all of them individually. Still a careful examination reveals that large changes in individual cross sections take place up to at least 50 eV, which have a strong influence on band shape. We report in Fig. 9 a series of profiles relative to the fourth band (gaussian width = 0.4 eV) evaluated at different photon energies, to illustrate the large change in the shape. Indeed in most experimental spectra a two peak structure is observed for band 4, although only a very narrow energy range (18.8–21.4 eV) has been studied in detail,[16] showing a large variation in the relative cross sections and a complete reversal in shape, supporting the present finding. A qualitative agreement with the observed behaviour can be seen in the profiles at 20 and 21 eV, where the intensity shifts completely from the low to the high energy component of the band.

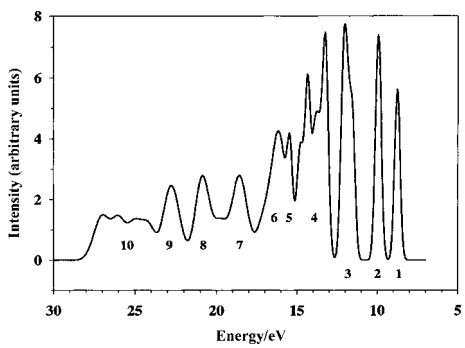

Fig. 8 Theoretical photoelectron spectrum simulated at 60 eV from calculated cross sections and WVN TS ionization potentials. Individual lines have been convoluted with gaussians of 0.4 eV FWHM up to band 5 and 1.0 eV width for the rest.

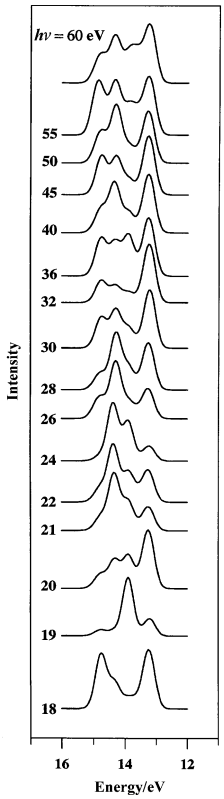

Fig. 9 Detail of the calculated shape of band 4 at various photon energies, employing calculated cross sections and ionization potentials. Individual lines have been convoluted with gaussians of 0.4 eV FWHM.

Finally, an important test of the calculated results is the comparison with the experimental data for the total cross section. This is illustrated in Fig. 10 with the total ion yield spectrum of Hertel *et al.*[17] shown as an inset. As has been previously underlined, interchannel coupling, as described at the SCI, RPA or TDLDA levels,[29–31] has a rather strong influence on the absorption spectrum, especially below and close to threshold. This is probably reflected in the too steep rise of the calculated spectrum at threshold, although the overall structure and span of the huge absorption resonance is in good agreement with the experimental result. Notably the data[17] have been renormalized to absolute values in ref. 41, and show a maximum of about 1200 Mb around 20 eV, in very good agreement with the present data. The full absorption spectrum of C_{60} has been carefully reexamined by Berkowitz,[41] who has critically assessed all available experimental data, which are widely scattered. His best evaluation of the spectrum is somewhat higher and wider than that of ref. 17, having a maximum around 1400 Mb at 22 eV, and a slower decay at the high energy side. However, in the discussion based on sum rules, a reduction of the cross section of about 22% is proposed to improve agreement, giving again a good match with the calculated values. A single experimental point is available at 40.8 eV,[24] in excellent agreement with the calculated value, and only the results of the calculated total cross section of 60 C atoms are available at higher energies. The present results fit nicely those values (Fig. 10) especially at higher energy, still showing many small jumps in the cross section which are of molecular origin, a kind of extended fine structure in the valence region. It is also interesting to note that the spectrum,[17] as discussed by Berkowitz,[41] falls more

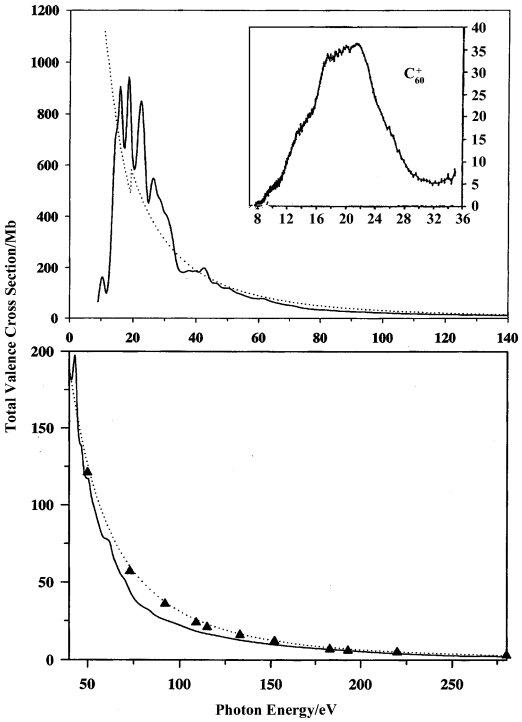

Fig. 10 Calculated total valence cross section. Dotted line is 60 × the carbon atomic cross section evaluated at the same level. The inset shows experimental total ion yield spectrum from ref. 17. Lower panel: enlargement of the high energy region, the filled triangles are atomic values from ref. 41.

steeply than that obtained by extrapolation of the atomic cross section from the high energy side, and the single point at 40.8, and would then require an almost constant cross section between 30–40 eV. This is, however, precisely what is shown by the present results, which give strong support to the data of Hertel *et al.*[17]

The atomic cross section (60 times the C cross section evaluated at the present LDA level) is reported as a dotted line in Fig. 10. It agrees very well at high energy with the values reported in ref. 41. Even in the low energy part it is striking to observe that, apart from the structure which is the essence of the molecular effect, it predicts the total cross section pretty well, the major effect of molecular formation being to transfer oscillator strength from threshold and from the region above 30 eV concentrating it in the spectral region between 15 and 30 eV. The good large scale match is naturally due both to conservation of the atomic character and to the constraints of sum rules.

Core region

In earlier studies on small systems,[39] as well as in C_6H_6,[46] we have observed that a good reproduction of the core photoemission spectrum is obtained by employing the same LB94 GS potential, even in the case of equivalent core holes. Despite the relatively slow convergence of C 1s eigenvalues in the one-center expansion, we have also found that cross sections and asymmetry parameters converge much faster, and full convergence is indeed attained in C_{60}. The results for the total C 1s cross section and angular distribution are reported in Fig. 11, and are compared with experimental data[20,25,41] in Fig. 12, where a smoothed profile (convoluted with a gaussian of 1.2 eV width) is employed. Again the presence of extremely sharp structures is surprising, although these are much broadened in the experimental spectrum. Individual features come from resonances obtained at different photoelectron kinetic energies in the different channels, which are available to dipole transitions for different symmetry combinations of

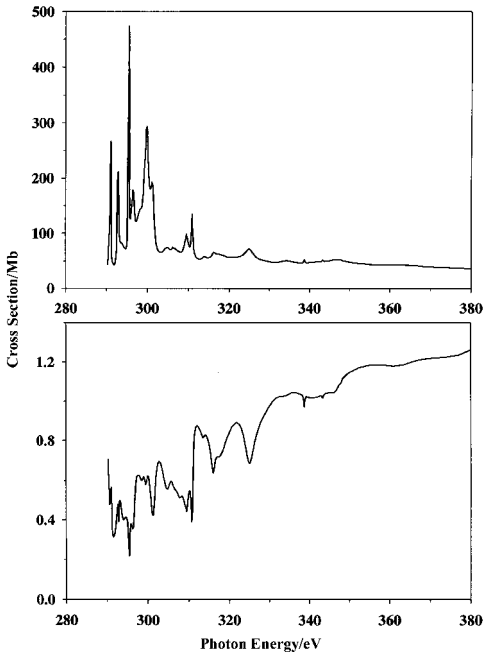

Fig. 11 Calculated total cross section (upper panel) and average asymmetry parameter (lower panel) relative to C 1s ionization. The experimental potential, IP = 290.1 eV[20] has been employed for all ionizations.

C 1s initial orbitals, and so are sensitive to the full molecular symmetry. Alternatively they could be considered as interference patterns from individual waves emitted by each individual C 1s orbital. The comparison of the cross section with the experimental spectrum normalized on an absolute scale[41] (Fig. 12, upper panel) is qualitatively correct, as most features seen experimentally have a good match in the calculated spectrum, as well as the maximum at around 10 eV above threshold, so that agreement is quite satisfactory. Actually the calculated cross section at the maximum is about twice as large as that estimated in ref. 41. However, the simulated

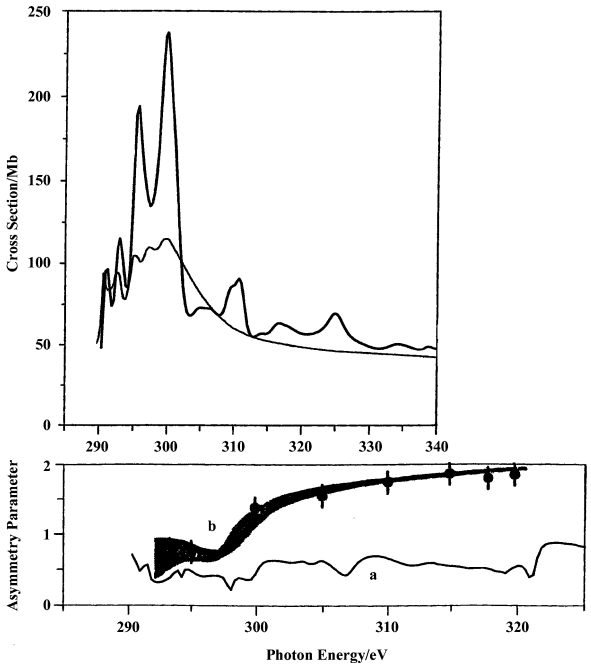

Fig. 12 Comparison of the calculated cross section (upper panel) and average angular distribution (part a in the lower panel), smoothed by convolution with a gaussian of 1.2 eV FWHM and the experimental data from ref. 41 (cross section) and 20 (asymmetry parameter, b in lower panel).

peaks are still much sharper than experimentally found, so that further broadening could reduce the value closer to that proposed in ref. 41, obtained by matching with the atomic cross section at the high energy side of the available data. Indeed the agreement at higher energy becomes quite satisfactory, with a calculated cross section $\sigma \approx 50$ Mb at 340 eV and an estimated value around 10% lower. However, in this case the calculated spectrum is consistently higher than the estimated one, and we suspect that the latter should probably be revised towards higher values. A significant structure is still calculated around 310 eV, a region however barely reached by the actual experimental measurement, and another one at 330 eV, so that no definite conclusion can be reached at the moment, but suggesting again that fitting with an atomic tail around 310 eV may be inadequate, and the experimental measurement should be carried out more than 50 eV above the threshold to achieve the atomic asymptotic limit.

The calculated β profile oscillates around the value 0.5 in the region of the experiment, then slowly increases (Fig. 12, lower panel). The experimental result[20] instead reaches quickly a much higher value, so that a significant discrepancy is observed there. From our previous study of C_6H_6 we have found a good qualitative agreement for β profiles when observed over a larger energy range, while the detail of the low energy part is often less satisfactory. Clearly a better evaluation of the present results requires more extensive experimental data.

Conclusions

The present method has been able to give a realistic description of the entire photoionization spectrum of C_{60}. Agreement with the available experimental data is quite satisfactory, and it is expected that the prediction of strong resonances and large cross section variations up to rather high photon energies are at least qualitatively correct, and should be observable in a more detailed analysis of photoelectron spectra. This in turn will drive a corresponding enhancement in the theoretical description, as is well illustrated by the quantitative comparison possible in the case of the HOMO/HOMO-1 ratio and of the total photoabsorption over an extended energy range. The presence of several sharp resonances in the core region is mirrored by corresponding structures in the experimental spectrum, but needs further confirmation. It is attributed to the presence of many symmetry distinct final channels available and the high centrifugal barrier which prevents decay of the antibonding excitations in the nonresonant continuum, both associated with the exceptional symmetry of C_{60}.

Acknowledgements

The authors are grateful to Professor S. Hasegawa for providing numerical data of the experimental and theoretical results of refs. 21 and 22 relative to the HOMO/HOMO-1 ratio.

This work was supported by grants from MURST of Italy and CNR of Rome (Italy). A generous grant of computer time on the CRAY T3E of CINECA (Bologna) is gratefully acknowledged.

References

1 R. C. Haddon, L. E. Brus and K. Raghavachari, *Chem. Phys. Lett.*, 1986, **125**, 459.
2 R. L. Disch and J. M. Schulman, *Chem. Phys. Lett.*, 1986, **125**, 465.
3 P. W. Fowler and J. Woolrich, *Chem. Phys. Lett.*, 1986, **127**, 78.
4 M. Ozaki and A. Takahashi, *Chem. Phys. Lett.*, 1986, **127**, 242.
5 S. Satpathy, *Chem. Phys. Lett.*, 1986, **130**, 545.
6 P. D. Hale, *J. Am. Chem. Soc.*, 1986, **108**, 6087.
7 J. L. Martins, N. Troullier and J. H. Weaver, *Chem. Phys. Lett.*, 1991, **180**, 457.
8 J. H. Weaver, J. L. Martins, T. Komeda, Y. Chen, T. R. Ohno, G. H. Kroll, N. Troullier, R. E. Haufler and R. E. Smalley, *Phys. Rev. Lett.*, 1991, **66**, 1741.
9 N. Troullier and J. L. Martins, *Phys. Rev. B*, 1992, **46**, 1754.
10 A. H. H. Chang, W. C. Ermler and R. M. Pitzer, *J. Phys. Chem.*, 1991, **95**, 9288.
11 B. I. Dunlap, D. W. Brenner, J. W. Mintmire, R. C. Mowery and C. T. White, *J. Phys. Chem.*, 1991, **95**, 8737.
12 J. W. Mintmire, B. I. Dunlap, D. W. Brenner, R. C. Mowery and C. T. White, *Phys. Rev. B*, 1991, **43**, 14281.
13 M. C. Böhm, J. Schulte and S. Philipp, *Chem. Phys. Lett.*, 1994, **226**, 381.
14 Y. Takahata, T. Hara, S. Narita and T. Shibuya, *J. Mol. Struct. (Theochem.)*, 1998, **431**, 219.
15 D. L. Lichtenberger, K. W. Nebesny, C. D. Ray, D. R. Huffman and L. D. Lamb, *Chem. Phys. Lett.*, 1991, **176**, 203.
16 P. J. Benning, D. M. Poirier, N. Troullier, J. L. Martins, J. H. Weaver, R. E. Haufler, L. P. F. Chibante and R. E. Smalley, *Phys. Rev. B*, 1991, **44**, 1962.
17 I. V. Hertel, H. Steger, J. De Vries, B. Weisser, C. Menzel, B. Kamke and W. Kamke, *Phys. Rev. Lett.*, 1992, **68**, 784.
18 S. Krummacher, M. Biermann, M. Neeb, A. Liebsch and W. Eberhardt, *Phys. Rev. B*, 1993, **48**, 8424.
19 H. Werner, Th. Schedel-Niedrig, M. Wohlers, D. Herein, B. Herzog, R. Schlögl, M. Keil, A. M. Bradshaw and J. Kirschner, *J. Chem. Soc., Faraday Trans.*, 1994, **90**, 403.
20 T. Liebsch, O. Plotzke, F. Heiser, U. Hergenhahn, O. Hemmers, R. Wehlitz, J. Viefhaus, B. Langer, S. B. Whitfield and U. Becker, *Phys. Rev. A*, 1995, **52**, 457.
21 S. Hasegawa, T. Miyamae, K. Yakushi, H. Inokuchi, K. Seki and N. Ueno, *Phys. Rev. B*, 1998, **58**, 4927.
22 S. Hasegawa, T. Miyamae, K. Yakushi, H. Inokuchi, K. Seki and N. Ueno, *J. Electron. Spectrosc.*, 1998, **88**, 891.
23 A. Rüdel, R. Hentges and U. Becker, *AIP Conf. Proc.*, 2000, **506**, 217.
24 R. F. Yoo, B. Ruscic and J. Berkowitz, *J. Chem. Phys.*, 1992, **96**, 911.
25 B. S. Itchkawitz, J. P. Long, Th. Schedel-Niedrig, M. N. Kabler, A. M. Bradshaw, R. Schlögl and W. R. Hunter, *Chem. Phys. Lett.*, 1995, **243**, 211.
26 L. L. Lohr and S. M. Blinder, *Chem. Phys. Lett.*, 1992, **198**, 100.
27 Y. B. Xu, M. Q. Tan and U. Becker, *Phys. Rev. Lett.*, 1996, **76**, 3538.
28 O. Frank and J.-M. Rost, *Chem. Phys. Lett.*, 1997, **271**, 367.
29 S. Larsson, A. Volosov and A. Rosén, *Chem. Phys. Lett.*, 1987, **137**, 501.
30 G. F. Bertsch, A. Bulgac, D. Tománek and Y. Wang, *Phys. Rev. Lett.*, 1991, **67**, 2690.
31 F. Alasia, R. A. Broglia, H. E. Roman, Ll. Serra, G. Colò and J. M. Pacheco, *J. Phys. B: At. Mol. Opt. Phys.*, 1994, **27**, L643.
32 K. Yabana and G. F. Bertsch, *Int. J. Quantum Chem.*, 1999, **75**, 55.
33 M. Venuti, M. Stener and P. Decleva, *Chem. Phys.*, 1998, **234**, 95.
34 M. Venuti, M. Stener, G. DeAlti and P. Decleva, *J. Chem. Phys.*, 1999, **111**, 4589.
35 R. R. Lucchese, F. A. Gianturco and N. Sanna, *Chem. Phys. Lett.*, 1999, **305**, 413.
36 F. A. Gianturco, R. R. Lucchese and N. Sanna, *J. Phys. B: At. Mol. Opt. Phys.*, 1999, **32**, 2181.
37 F. A. Gianturco and R. R. Lucchese, *J. Chem. Phys.*, 1999, **111**, 6769.
38 F. A. Gianturco and R. R. Lucchese, *Phys. Rev. A*, 1999, **60**, 4567.
39 M. Stener, S. Furlan and P. Decleva, *J. Phys. B: At. Mol. Opt. Phys.*, 2000, **33**, 1081.
40 R. van Leeuwen and E. J. Baerends, *Phys. Rev. A*, 1994, **49**, 2421.
41 J. Berkowitz, *J. Chem. Phys.*, 1999, **111**, 1446.
42 E. J. Baerends, D. E. Ellis and P. Ros, *Chem. Phys.*, 1973, **2**, 41.
43 M. Brosolo and P. Decleva, *Chem. Phys.*, 1992, **159**, 185.
44 D. Dill and J. L. Dehmer, in *Electron–Molecule and Photon–Molecule Collisions*, ed. T. Rescigno, V. McKoy and B. Schneider, Plenum, New York, 1979, p. 225.
45 M. B. Robin, *Chem. Phys. Lett.*, 1985, **119**, 33.
46 M. Stener, S. Furlan and P. Decleva, *Phys. Chem. Chem. Phys.*, 2001, **3**, 19.